Nuclear Physics A405 (1983) 170–178

^{25}Mg (α, n)^{28}Si AND ^{26}Mg(α, n)^{29}Si AS NEUTRON SOURCES IN EXPLOSIVE NEON BURNING†

M. R. ANDERSON††, L. W. MITCHELL, M. E. SEVIOR and D. G. SARGOOD

School of Physics, University of Melbourne, Parkville, Victoria 3052, Australia

Received 8 February 1983
(Revised 28 March 1983)

Abstract: The yields of neutrons from the reaction ^{25}Mg(α, n)^{28}Si and of γ-rays from the reaction ^{25}Mg(α, nγ)^{28}Si have been measured as a function of bombarding energy over the range 1.8–6.3 MeV, and the yield of neutrons from ^{26}Mg(α, n)^{29}Si has been measured over the range 1.8–6.0 MeV. Cross sections for ^{25,26}Mg(α, n)^{28,29}Si were extracted from the data and compared with global statistical-model calculations. The agreement is very good. Thermonuclear reaction rates under stellar conditions appropriate for explosive neon burning are calculated and their significance for the nucleosynthesis of rare neutron-rich nuclei is discussed.

E | NUCLEAR REACTIONS ^{25}Mg(α, n), (α, nγ), E = 1.8–6.3 MeV; ^{26}Mg(α, n), E = 1.8–6.0 MeV; measured neutron and γ-ray yields; deduced $\sigma(E)$, thermonuclear reaction rates. Statistical-model analysis. Enriched targets.

1. Introduction

Howard *et al.* [1]) have shown that many rare neutron-rich nuclei, which are bypassed by the mainstream of nucleosynthesis in evolving and exploding stars, can be produced on an explosive time scale in an environment in which there is initially a short-lived high flux of neutrons followed by a high flux of free protons. During the neutron phase, chains of rapid neutron captures by seed nuclei, which are the products of oxygen burning in earlier generation stars, lead to the production of highly neutron-rich matter in a fashion similar to that of the r-process of Burbridge *et al.* [2]). The process differs from the r-process in that the subsequent reduction in neutron enrichment of nuclei occurs not by β-decays but by (p, n) reactions during the proton phase, so there is no net change in the neutron enrichment of the fuel. The site proposed by Howard *et al.* [1]) for their process was that of explosive carbon burning at a temperature of T_9 = 2–2.15,

† Supported in part by the Australian Research Grants Scheme (B77/15413).
†† Present address: Mineral Physics Division, CSIRO, 339 Williamstown Road, Port Melbourne, Victoria 3207, Australia.

where T_9 is the temperature in units of 10^9 K, but more recent calculations by Arnett and Wefel [3]), Weaver and Woosley [4]), and Woosley and Weaver [5]) raise serious doubts as to whether explosive carbon burning occurs at all. However, these calculations indicate that some of the ashes of hydrostatic carbon burning do undergo explosive neon burning and Woosley and Weaver [6]) have discussed this process for peak temperatures up to $T_9 = 3$. It is therefore worth considering the explosive neon-burning shell of a supernova as a possible alternative site for the process of Howard *et al.* [1]) but, whereas Howard *et al.* assumed the main source of free neutrons in carbon burning to be $^{18}O(\alpha, n)^{21}Ne$, the main sources in neon burning are likely to be $^{25}Mg(\alpha, n)^{28}Si$ and $^{26}Mg(\alpha, n)^{29}Si$. We therefore decided to measure the cross sections for these two reactions over the energy ranges important in determining stellar reaction rates for $T_9 = 1.5$–3, a temperature range which should cover the whole of the neutron phase of the Howard *et al.* process.

As is the case with all measurements of reaction cross sections over extended energy ranges, these measurements also provide additional data to compare with the predictions of statistical-model codes. Such comparisons are important for nucleosynthesis calculations because these calculations depend heavily on theoretical cross sections, and it is important to establish the reliability of the statistical-model codes used in generating them.

2. Experimental procedures

2.1. TARGETS

Targets were prepared by evaporation from an intimate mixture of isotopically enriched magnesium oxide and tantalum powder, in a mass ratio of 1 : 20, on to tantalum backings. The ^{25}Mg targets were enriched to 97.87 % in ^{25}Mg and the ^{26}Mg targets to 99.70 % in ^{26}Mg.

The ^{25}Mg target thickness was measured by comparison of the observed integrated γ-ray yields from the 433 and 592 keV resonances in $^{25}Mg(p, \gamma)^{26}Al$ with those calculated from the published resonance strength values of 1.17 ± 0.09 and 2.74 ± 0.20 eV, respectively [7]).

The ^{26}Mg target thickness was measured in a similar manner by way of the 1966 keV resonance in $^{26}Mg(p, \gamma)^{27}Al$ and the published value of 10.3 ± 0.9 eV for its resonance strength [8])

The γ-ray yields were measured with a 60 cm^3 Ge(Li) detector located 8 cm from the target in the 125° direction and calibrated by means of standard sources and the 2046 keV resonance in $^{27}Al(p, \gamma)^{28}Si$ [ref. [9])]. In the analysis of the γ-ray yield data the branching ratios of refs. [10,11]) were used, and since angular distribution measurements of refs. [10,12]) showed any $P_4(\cos\theta)$ terms to be negligible, no correction was made for angular distribution effects.

The adopted values for target thicknesses were $(7.56 \pm 0.77) \times 10^{17}$ ^{25}Mg

atoms $\cdot$ cm^{-2} and $(6.76 \pm 0.74) \times 10^{17}$ ^{26}Mg atoms $\cdot$ cm^{-2}. The target thickness measurements were made before and after the (α, n) measurements and no target deterioration was observed.

2.2. THE REACTION $^{25}Mg(\alpha, n)^{28}Si$

The ^{25}Mg target was bombarded with α-particles of energy 1.8–6.0 MeV delivered by the Melbourne 5U Pelletron accelerator. The beam was collimated and passed through an electron suppression ring held at -600 V before entering the target chamber which was insulated and used as a Faraday cup. The energy was increased in steps of 50 keV, the energy thickness of the target at ~ 2 MeV, and target currents were typically ~ 0.3 μA for energies below 5 MeV, where the beam consisted of the He^+ ions, and ~ 20 nA for energies above 5 MeV, where the beam consisted of He^{++} ions. At each energy a clean tantalum blank was also bombarded to give a measurement of background.

Neutrons were detected with a detector consisting of four BF_3 tubes of active length 40 cm embedded in a cube of paraffin of side 50 cm, with the target at its centre. The tubes were symmetrically arranged parallel to the beam direction and their centres were 17 cm from the target. A cavity cut into the paraffin permitted the location of a 60 cm^3 Ge(Li) detector 8 cm from the target in the 125° direction, for use in detection efficiency measurements and in $(\alpha, n\gamma)$ measurements. The detection efficiency was measured by means of calibrated Am-F, Am-B and Am-Be sources, and the reactions ^{7}Li(p, n)^{7}Be, ^{48}Ca(p, n)^{48}Sc, and ^{50}Ti(p, nγ)^{50}V, as described in ref. [13]). The detection efficiency was constant at (3.16 ± 0.25) % for neutrons of energy 0.7–7.0 MeV and, as shown by the ^{50}Ti(p, nγ)^{50}V measurements, fell linearly at lower energies with a zero energy intercept of 1.8 %. Statistical-model calculations indicated that > 85 % of neutrons from $^{25}Mg(\alpha, n)^{28}Si$ would have energies in the range 0.7–7.0 MeV for our α-particle energy range, indicating that any errors associated with corrections to the detection efficiency for neutron energies below 0.7 MeV would be small.

Further statistical-model calculations indicated that the neutron yield would lead to ^{28}Si excited states the γ-ray decay schemes of which give rise to the 1779 keV $1 \rightarrow$ g.s. transition with 75 % probability for an α-particle energy of 1.8 MeV, rising smoothly to 94 % for an α-particle energy of 6.3 MeV. The excitation function measurement was therefore repeated with the 1779 keV γ-ray being detected by means of the Ge(Li) detector, concurrently with the neutron yield measurements. This measurement was made with energy steps of 100 keV over the energy range 2.1–6.3 MeV. For bombarding energies below 2.1 MeV poor statistics on the γ-ray peak made it necessary to move the Ge(Li) detector closer to the target. A separate excitation function of $^{25}Mg(\alpha, n\gamma_1)^{28}Si$ was therefore measured with a target chamber which permitted the location of the Ge(Li) detector 2 cm from the target in the 55° direction. This measurement covered the

energy range 1.8–2.45 MeV in 50 keV steps. Agreement between the two excitation functions in the region of overlap was within statistics at all points. For bombarding energies above 2.8 MeV the yield of 1779 keV γ-rays was enhanced by a contribution from $^{25}Mg(\alpha, p)^{28}Al(\beta^-\gamma)^{28}Si$. This radioactive yield was therefore measured over a 5 m counting period before and after each point in the excitation function and the contribution to each point due to the 2.24 m ^{28}Al activity was determined by standard activation methods. The run time for each point was $\sim$ 5 m and the beam current was constant to ± 10 %. Since the correction for the activity never exceeded 10 %, we estimate the contribution to overall errors at $\sim$ 1 %.

2.3. THE REACTION $^{26}Mg(\alpha, n)^{29}Si$

An excitation function for $^{26}Mg(\alpha, n)^{29}Si$ was measured over the energy range 2.1–6.0 MeV in 50 keV steps, the neutrons being detected with the neutron detector already described. For lower α-particle energies statistical-model calculations predicted that a significant fraction of the neutron yield would be at energies below 0.7 MeV, the lower limit of the flat response of the neutron detector. A second neutron detector was therefore constructed with a flat response for neutron energies in the range 0–2 MeV. Owing to failure of one of the BF_3 tubes, this detector eventually contained only two tubes which were embedded in a rectangular block of paraffin 15 cm $\times$ 27 cm $\times$ 50 cm, with the target located at the centre of one 27 cm $\times$ 50 cm face and 6.3 cm from the BF_3 tubes. Between the 27 cm $\times$ 50 cm faces there was centrally located a cavity 7 cm $\times$ 27 cm $\times$ 15 cm, as a result of which the probability of absorption of low-energy neutrons in the paraffin was greatly reduced and the low-energy detection efficiency correspondingly increased. The detection efficiency was constant at (3.15 ± 0.30) % over the neutron energy range 0–2 MeV. An excitation function was measured with this detector over the energy range 1.8–2.4 MeV. Agreement between the excitation functions measured with the two neutron detectors was within statistics in the region of overlap.

3. Results and discussion

3.1. THE REACTION $^{25}Mg(\alpha, n)^{28}Si$

The $^{25}Mg(\alpha, n)^{28}Si$ results are plotted in fig. 1. The open circles are cross sections derived from the neutron detector data and the crosses are derived from the Ge(Li) detector measurements of $^{25}Mg(\alpha, n\gamma_1)^{28}Si$. The $(\alpha, n\gamma_1)$ yield data were converted to (α, n) total yields on the basis of (α, n_i) branching ratios calculated with the statistical-model code HAUSER*4 [ref. [14])] and the γ-ray branching ratios of ref. [15]).

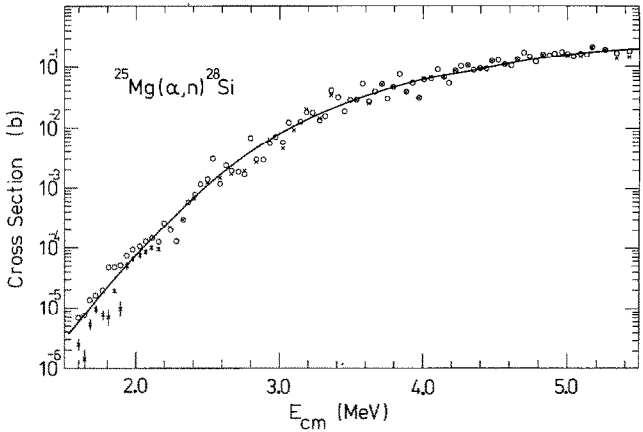

Fig. 1. Excitation function for $^{25}Mg(\alpha, n)^{28}Si$. The circles correspond to cross sections deduced from direct observation of neutrons and the crosses to cross sections deduced from observation of γ-rays from $^{25}Mg(\alpha, n\gamma)^{28}Si$. Error bars reflect statistical uncertainties only: where not shown, they are of the order of the size of the plotted points. The curve represents the statistical-model calculation of the code HAUSER*4.

At energies above $E_{c.m.} = 2.5$ MeV the background corrections to the neutron detector data were typically ~ 1 % and always < 3 %. However, at lower energies the background became a rapidly increasing fraction of the total neutron yield and the results obtained by subtracting it became increasingly dubious. At $E_{c.m.} < 2.4$ MeV it became clear from the γ-ray spectra that $^{18}O(\alpha, n\gamma)^{21}Ne$ and $^{19}F(\alpha, n\gamma)^{22}Na$ were significant contaminant sources of neutrons. The γ-ray yields from these contaminant reactions were much weaker during the background runs on the tantalum blank, indicating that the impurities were mainly in the target itself, and revealing further deficiencies in the background subtraction procedure. Additional corrections for the neutron yield due to the $(\alpha, n\gamma)$ reactions were made on the basis of the γ-ray yield but the reactions $^{19}F(\alpha, n_0)^{22}Na$ and $^{18}O(\alpha, n_0)^{21}Ne$, and possibly $^{13}C(\alpha, n_0)^{16}O$, went unobserved. Hence the corrected neutron yields represent an upper limit to those from $^{25}Mg(\alpha, n)^{28}Si$, with probable significant contributions from these contaminant reactions at energies below ~ 2 MeV.

The excellent agreement between the corrected (α, n) and $(\alpha, n\gamma)$ results for $E_{c.m.} \geqq 2.4$ MeV is gratifying and lends support to the reliability of both methods of measuring the neutron yield. For $E_{c.m.} < 2.2$ MeV the (α, n) results are consistently higher than the $(\alpha, n\gamma)$ results and, since the $(\alpha, n\gamma)$ measurements were not subject to the background-subtraction problems affecting (α, n), the cross sections based on the $(\alpha, n\gamma)$ observations are the more reliable and are therefore the data to be used for comparison with statistical-model calculations and for calculation of thermonuclear reaction rates.

The curve in fig. 1 represents the cross section as calculated by the code

HAUSER*4. The absolute error associated with the experimental cross section is estimated at 12 % with the main contributions coming from target thickness, 10 %, and Ge(Li) detector efficiency, 6 %. The level of agreement between the results of HAUSER*4 and the experimental cross sections, averaged over a 0.5 MeV energy interval, is within this 12 % limit over almost the entire energy range. This is a most impressive achievement for the code.

3.2. THE REACTION $^{26}Mg(\alpha, n)^{29}Si$

The $^{26}Mg(\alpha, n)^{29}Si$ results are plotted in fig. 2. The curve again represents the cross section as calculated by the code HAUSER*4. The level of agreement is very good, particularly for $E_{c.m.} > 2$ MeV: the curve is 7 % below the averaged data in the energy range 2–3 MeV, 20 % below in the range 3–4 MeV, and 33 % below in the range 4–5 MeV. The error associated with the experimental data is 14 % with the main contributors being target thickness, 11 %, and detector efficiency, 8 %. The performance of HAUSER*4 is therefore very good for a code which uses global optical-model parameters for the calculation of transmission functions. For $E_{c.m.}$ below ~ 2.2 MeV, we were guided by our experience with $^{25}Mg(\alpha, n)^{28}Si$ to regard the experimental points as upper limits and therefore do not consider the fact that the statistical model curve falls consistently below the data for $E_{c.m.} < 2$ MeV to be significant.

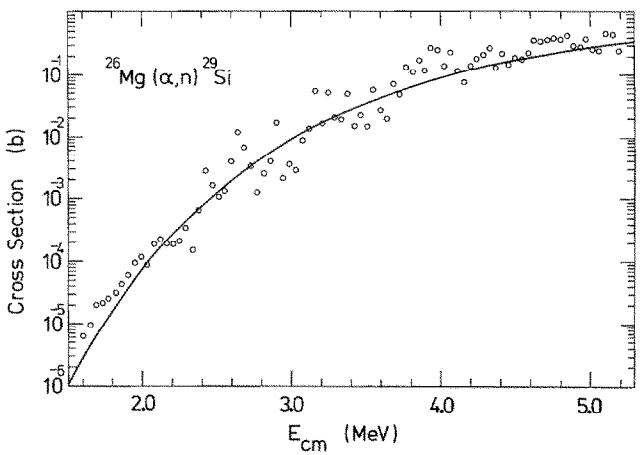

Fig. 2. Excitation function for $^{26}Mg(\alpha, n)^{29}Si$. Statistical error bars are of the order of the size of the plotted points. The curve represents the statistical-model calculation of the code HAUSER*4.

4. Thermonuclear reaction rates

The thermonuclear reaction rate per mole is the product of Avogadro's number, N_A, and the thermally averaged product, $\langle \sigma v \rangle$, of the cross section and the relative velocity of the interacting particles. Fowler *et al.* [16]) give the expression

$$\langle \sigma v \rangle^0 = (8/\pi M)^{\frac{1}{2}} (kT)^{-\frac{3}{2}} \int_0^\infty \sigma(E) E \exp(-E/kT) \mathrm{d}E,$$

where M is the reduced mass, E is the c.m. energy, and the superscript zero indicates that the target is in its ground state. We have used this expression to calculate $N_A \langle \sigma v \rangle^0$, as a function of temperature, for each of $^{25}Mg(\alpha, n)^{28}Si$ and $^{26}Mg(\alpha, n)^{29}Si$.

For $^{25}Mg(\alpha, n)^{28}Si$, the cross sections used in the calculation were the average of those derived from the neutron detector and Ge(Li) detector measurements for $E_{c.m.} > 2.2$ MeV, and those derived from the Ge(Li) detector alone for $E_{c.m.} < 2.2$ MeV. When cross sections were needed for energies above or below the experimental range these were calculated by means of HAUSER*4. The excellent fit of the HAUSER*4 excitation function to the experimental data gave us considerable confidence in the use of these calculated cross sections. The contributions of HAUSER*4 cross sections to the thermonuclear reaction rates were 12 % at $T_9 = 1.5$ and < 10 % for $T_9 = 1.6$–5.5, rising to 40 % at $T_9 = 10$.

For $^{26}Mg(\alpha, n)^{29}Si$ we were guided by the $^{25}Mg(\alpha, n)^{28}Si$ data in deciding that the experimental cross sections were reliable down only to $E_{c.m.} = 2.2$ MeV, and used HAUSER*4 calculated cross sections for all energies below this. The quality of the fit of the HAUSER*4 excitation function to the experimental data, particularly in the energy range $E_{c.m.} = 2$–3 MeV, again gave us confidence in this procedure. However, the structure which is evident in the excitation function indicates that the basic high level density assumption of the statistical model is less well satisfied for $^{26}Mg(\alpha, n)^{29}Si$ than for $^{25}Mg(\alpha, n)^{28}Si$, and the use of HAUSER*4 should accordingly be treated with more caution. The contributions of HAUSER*4 cross sections to the thermonuclear reaction rates were 40 % at $T_9 = 1.5$, and < 10 % for $T_9 = 2.1$–5.2, rising to 50 % at $T_9 = 10$.

Under stellar conditions nuclei are thermally excited into excited states, and we have converted our values of $N_A \langle \sigma v \rangle^0$ to $N_A \langle \sigma v \rangle^*$, the thermonuclear reaction rate appropriate to a stellar environment, by multiplying them by the ratio $\langle \sigma v \rangle^* / \langle \sigma v \rangle^0$ of Woosley *et al.* [17]), which is based on the assumption of a thermal distribution of excited states.

Our values of $N_A \langle \sigma v \rangle^0$ and $N_A \langle \sigma v \rangle^*$ are listed in table 1 as a function of temperature, along with the values of $N_A \langle \sigma v \rangle^*$ of ref. [17]) for comparison. The ratio of the values of $N_A \langle \sigma v \rangle^*$ of ref. [17]) to those of the present work ranges from 1.7 at $T_9 = 1.5$ to 1.2 at $T_9 = 5$–10 for $^{25}Mg(\alpha, n)^{28}Si$, and from 1.2 at $T_9 = 1.5$ to 0.8 at $T_9 = 5$ and 0.5 at $T_9 = 10$ for $^{26}Mg(\alpha, n)^{29}Si$. These

TABLE 1

Thermonuclear reaction rates ($cm^3 \cdot s^{-1} \cdot mole^{-1}$)

T_9	$^{25}Mg(\alpha, n)^{28}Si$			$^{26}Mg(\alpha, n)^{29}Si$		
	$N_A\langle\sigma v\rangle^0$ this work	$N_A\langle\sigma v\rangle^*$		$N_A\langle\sigma v\rangle^0$ this work	$N_A\langle\sigma v\rangle^*$	
		this work	ref. [17])		this work	ref. [17])
1.5	2.21×10^{-1}	2.21×10^{-1}	3.74×10^{-1}	3.27×10^{-1}	3.27×10^{-1}	3.90×10^{-1}
1.6	5.49×10^{-1}	5.49×10^{-1}		7.75×10^{-1}	7.75×10^{-1}	
1.8	2.72	2.72		4.28	4.28	
2.0	1.06×10	1.06×10	1.61×10	1.72×10	1.72×10	1.71×10
2.2	3.46×10	3.46×10		5.77×10	5.77×10	
2.5	1.53×10^2	1.53×10^2	2.14×10^2	2.61×10^2	2.61×10^2	2.32×10^2
2.8	5.36×10^2	5.36×10^2		9.14×10^2	9.14×10^2	
3.0	1.10×10^3	1.10×10^3	1.43×10^3	1.89×10^3	1.89×10^3	1.59×10^3
3.5	5.01×10^3	4.97×10^3	6.13×10^3	8.57×10^3	8.57×10^3	7.01×10^3
4.0	1.64×10^4	1.62×10^4	1.95×10^4	2.88×10^4	2.88×10^4	2.29×10^4
4.5	4.26×10^4	4.18×10^4	4.99×10^4	7.63×10^4	7.63×10^4	6.00×10^4
5.0	9.50×10^4	9.24×10^4	1.09×10^5	1.74×10^5	1.74×10^5	1.34×10^5
6.0	3.26×10^5	3.14×10^5	3.70×10^5	6.19×10^5	6.15×10^5	4.73×10^5
7.0	8.28×10^5	7.87×10^5	9.24×10^5	1.61×10^6	1.58×10^5	1.21×10^6
8.0	1.70×10^6	1.59×10^6	1.88×10^6	3.36×10^6	3.25×10^6	2.51×10^6
9.0	3.04×10^6	2.78×10^6	3.29×10^6	6.09×10^6	5.68×10^6	4.40×10^6
10.0	4.89×10^6	4.37×10^6	5.15×10^6	9.92×10^6	8.79×10^6	4.40×10^6

values satisfy the frequently quoted aim of ref. [17]) to predict reaction rates correctly to within a factor of 2.

We have parametrised our values of $N_A\langle\sigma v\rangle^*$ according to eq. (8) of Woosley *et al.* [18]),

$$N_A\langle\sigma v\rangle^* = T_9^{-2/3} \exp\left[A - (\tau/T_9^{1/3})(1 + BT_9 + CT_9^2 + DT_9^3)\right],$$

where τ is given by eq. (25) of ref. [19]), A has been set equal to the value in the tabulation of Woosley *et al.* [18]) reduced by an amount equal to $\ln\{\langle\sigma v^*$ [ref. [17])]$/\langle\sigma v\rangle^*$ [present]$\}$ at $T_9 = 1.5$, and B, C, and D are treated as free parameters. The use of this value of A gives theoretical validity to the use of these parameter sets to calculate thermonuclear reaction rates at temperatures below $T_9 = 1.5$. The values of the parameters are listed in table 2. The $^{25}Mg(\alpha, n)^{28}Si$ parameter set fits the experimental rates to within 12 % for $T_9 = 1.5$–8 and 20 % for $T_9 = 8$–10. The $^{26}Mg(\alpha, n)^{29}Si$ set fits to within 10 % for $T_9 = 2$–10 and 20 % for $T_9 = 1.5$–2.

Howard *et al.* [1]) carried out their nucleonsynthesis calculations for a temperature of $T_9 = 2.15$, using the rate for their neutron-producing reaction, $^{18}O(\alpha, n)^{21}Ne$, as calculated according to the prescription of Couch and Arnett [20]). This rate, 3.38×10^3, is equal, within errors, to the weighted sum of the rates for

TABLE 2

Parameters for fits to stellar reaction rates

	$^{25}Mg(\alpha, n)^{28}Si$	$^{26}Mg(\alpha, n)^{29}Si$
τ	53.42	53.51
A	46.78	47.21
B	1.576×10^{-2}	1.455×10^{-2}
C	1.251×10^{-3}	9.879×10^{-4}
D	-8.124×10^{-5}	-5.020×10^{-5}

$^{25}Mg(\alpha, n)^{28}Si$ and $^{26}Mg(\alpha, n)^{29}Si$ at $T_9 = 3$ as reported here, the weighting factors being the natural abundances of ^{25}Mg and ^{26}Mg. Since the number density of ^{25}Mg plus ^{26}Mg after carbon burning is within an order of magnitude of that of ^{18}O before carbon burning [21]), it is clear that at $T_9 \sim 3$ the reactions $^{25}Mg(\alpha, n)^{28}Si$ and $^{26}Mg(\alpha, n)^{29}Si$ would produce a similar neutron flux to that from $^{18}O(\alpha, n)^{21}Ne$ at $T_9 = 2.15$ provided only that the free α-particle density is similar in both cases. It therefore appears that explosive neon burning may indeed provide a suitable neutron flux for the operation of the Howard *et al.* process.

References

1) W. M. Howard, W. D. Arnett, D. D. Clayton and S. E. Woosley, Astrophys. J. **175** (1972) 201
2) E. M. Burbidge, G. R. Burbidge, W. A. Fowler and F. Hoyle, Rev. Mod. Phys. **29** (1951) 547
3) W. D. Arnett and J. P. Wefel, Astrophys. J. **224** (1978) L139
4) T. A. Weaver and S. E. Woosley, Ann. NY Acad. Sci. **336** (1980) 335
5) S. E. Woosley and T. A. Weaver, in Essays in nuclear astrophysics, ed. C. A. Barnes, D. D. Clayton and D. N. Schramm (Cambridge University Press, Cambridge, 1982) p. 377
6) S. E. Woosley and T. A. Weaver, Astrophys. J. **238** (1980) 1017
7) M. R. Anderson, S. R. Kennett, L. W. Mitchell and D. G. Sargood, Nucl. Phys. **A349** (1980) 154
8) B. M. Paine and D. G. Sargood, Nucl. Phys. **A331** (1979) 389
9) D. L. Kennedy, J. C. P. Heggie, P. J. Davies and H. H. Boloton, Nucl. Instr. **140** (1977) 519
10) E. O. De Neijs, M. A. Meyer, J. P. L. Reineke and D. Reitmann, Nucl. Phys. **A230** (1974) 490
11) C. van der Leun, D. M. Sheppard and P. M. Endt, Nucl. Phys. **A100** (1967) 316
12) D. M. Sheppard and C. van der Leun, Nucl. Phys. **A100** (1967) 316
13) D. G. Sargood, Phys. Reports **93** (1982) 61
14) F. M. Mann, Hanford Engineering Development Lab. report HEDL-TME-7680 (1976), unpublished
15) M. A. Meyer, I. Venter and D. Reitmann, Nucl. Phys. **A250** (1975) 235
16) W. A. Fowler, G. R. Coughlan and B. A. Zimmerman, Ann. Rev. Astr. Astrophys. **5** (1967) 525
17) S. E. Woosley, W. A. Fowler, J. A. Holmes and B. A. Zimmerman, Caltech preprint OAP-422 (1975), unpublished
18) S. E. Woosley, W. A. Fowler, J. A. Holmes and B. A. Zimmerman, Atom. Nucl. Data Tables **22** (1978) 371
19) J. A. Holmes, S. E. Woosley, W. A. Fowler and B. A. Zimmerman, Atom. Nucl. Data Tables **18** (1967) 305
20) R. G. Couch and W. D. Arnett, Astrophys. J. **178** (1972) 771
21) W. D. Arnett and J. W. Truran, Astrophys. J. **157** (1969) 339